In Situ IR Study of the Anodic Polarization of Gold Electrodes in Polar Aprotic Solvents: DMSO and DMF Solutions of Cyanate, Thiocyanate and Selenocyanate Ions

Kethsiri H. K. L. Alwis and Michael R. Mucalo[z]

Chemistry, School of Science, University of Waikato, Hamilton 3240, New Zealand

Subtractively normalised Fourier transform infrared spectroscopic (SNIFTIRS) studies combined with volammetric and supporting model solution studies have conclusively shown that Au electrodes anodically polarized in DMSO and DMF solutions containing the pseudohalide ions: cyanate, thiocyanate and selenocyanate with tetrabutylammonium perchlorate as supporting electrolyte dissolve to form Au(I) pseudohalide complex ions (i.e. $[Au(NCO)_2]^-$, $[Au(SCN)_2]^-$ and $[Au(SeCN)_2]^-$. This work has demonstrated the significance of the Au(I) oxidation state which occurs after applied voltages of +500 mV(AgCl/Ag) in the little characterized electrochemistry of this metal in polar aprotic solvents, DMSO and DMF The Au(I) species observed electrochemically by SNIFTIRS were confirmed by independent preparation in DMSO/DMF containing mixtures of $KAuBr_4$ and the pseudohalide salt (KOCN/NaSCN/KSeCN) and exploiting fortuitous redox chemistry where Au(I) formed spontaneously. The model solutions examined by transmission FTIR and ESI-MS confirmed the existence of the Au(I) species posited in the SNIFTIRS experiments but additionally revealed other interesting side reactions occurring in the model solutions.

Manuscript submitted July 18, 2014; revised manuscript received August 13, 2014. Published August 20, 2014.

The study of the anodic dissolution of transition metal electrodes in polar aprotic solvents such as dimethyl sulfoxide (DMSO) and dimethyl formamide (DMF) containing pseudohalide salts is useful because these systems have only been studied to a small extent using electrochemical methods in the literature without any direct detection of electrically generated molecular species formed being made. Their investigation assists in understanding the electrochemical behavior of these metals in non-aqueous polar aprotic solvents (DMF or DMSO) which find use not only in various chemical industries[1–3] such as electrowinning but also refining of metals in these solvents. They may also allow comparisons of electrochemical behavior between aqueous based and non-aqueous based electrolytes. The importance of the chemistry of gold and its interaction with pseudohalide ions such as cyanide, thiocyanate, cyanate and selenocyanate cannot be overestimated given its relevance in areas such as the recovery and recycling of gold.[4] In addition, the reason for studying pseudohalide interactions with Au electrodes is because these ions mimic chemically the halide ions. Hence these ions can be exploited as spectroscopic probes to understand better electrochemical phenomena since the pseudohalide ions (viz., NCO^-, NCS^-, and $NCSe^-$) have an easily detectable IR signature (i.e. ν(CN) stretching vibrations) in the 2500–1800 cm^{-1} region of the IR spectrum which is relatively free from solvent-related spectral interferences. The combined use of infrared (IR) and dynamic electrochemistry techniques has provided a wealth of molecular information relating to oxidation, reduction and related processes occurring in situ at metal electrode/electrolyte interfaces.[5–24] Subtractively normalised interfacial Fourier transform infrared spectroscopy (SNIFTIRS) can elucidate the molecular species formed during anodic dissolution via detection of solution species electrogenerated in the thin layer of electrolyte between the working electrode and the IR window. SNIFTIRS has been regularly used in our laboratory for characterizing the electrochemistry of little studied systems such as the anodic polarization of transition metals (Ni) in the presence of pseudohalide ions dissolved either in aqueous solution[18] or, in DMF or DMSO solutions containing tetrabutylammonium perchlorate (TBAP) as a supporting electrolyte.[5]

The aim of the present study is hence to better understand the anodic polarization behavior and speciation of gold electrodes in the non-aqueous, polar aprotic solvents, DMSO or DMF containing pseudohalide ions such as NCO^-, NCS^- and $NCSe^-$ through the use of SNIFTIRS techniques. It is to be noted that most in situ IR work for these systems has been with aqueous electrolytes,[10–13,25] though Benari et al.[26] and Martins et al.[27,28] have studied anodic dissolution of gold in acetonitrile or DMSO containing thiocyanate ion but not by the use of in situ IR techniques. To aid in and confirm assignments made for molecular species generated in the electrochemical studies, model solutions were also made using Au(III) salts with added pseudohalide ions to synthesize the electrogenerated species independently of the electrochemical cell to prove their chemical existence via fortuitous redox chemistry occurring in some of these solutions. These model solutions were characterized by FTIR transmission spectroscopy and Electrospray Ionisation Mass Spectrometry (ESI-MS).

Materials and Methods

Reagents and solutions.— DMF and DMSO used in this study were sourced from Ajax Finechem Pty and Scharlau and used without further purification as described in an earlier publication.[5] All glassware was cleaned prior to beginning experiments with doubly distilled water and dried. Other reagents used being KOCN, NaSCN, KSeCN, $KAuBr_4$, gold foil (99.99%, 0.1 mm thick) and tetrabutylammonium perchlorate (TBAP) were supplied by Aldrich Chemical Co USA as previously described.[5] When used either as (DMSO/DMF) electrolyte solutions or in model solutions the concentration of the TBAP (used as an inert supporting electrolyte) was 0.1 mol L^{-1}. For the pseudohalide salts, the concentrations used were 0.025 mol L^{-1} in the case of potassium cyanate (owing to its limited solubility in the polar aprotic solvents used) and 0.05 mol L^{-1} in the case of the thiocyanate and selenocyanate salts.

Spectroelectrochemical cell and electrode design.— The thin layer cell used for this work has had details and illustrations published recently elsewhere.[5] The gold electrode was a flat, circular polycrystalline piece of gold of 0.1 mm thickness embedded in a glass syringe barrel using Araldite epoxy glue. The preparation of this electrode has been covered in an earlier reported work.[18] The gold electrode was polished using alumina paste.

Instrumentation.— As described previously,[5] cyclic voltammetry (CV) was acquired over the region of –800 to 2000 mV (AgCl/Ag) using an EDAQ computer controlled potentiostat system which was run using Echem software. A Radiometer "red

[z]E-mail: mucalo@waikato.ac.nz

rod" (AgCl/Ag) reference electrode was employed with a platinum metal ring utilised as the counter electrode. Typically a CV scan was run first of the electrochemical system under study these being: Au/DMSO/NCO^-, Au/DMSO/NCS^-, Au/DMSO/$NCSe^-$, Au/DMF/NCO^-, Au/DMF/NCS^-, and Au/DMF/$NCSe^-$. In situ IR (SNIFTIRS) spectra were acquired using a Biorad FTS-40 FTIR spectrometer equipped with a liquid N_2-cooled indium antimonide (InSb) detector as previously indicated.[5] In situ IR spectra were normally acquired at 4 cm^{-1} resolution as the accumulation of 100 scans at different potentials above the background potential where the background spectrum used was that of the thin layer created when the polished gold electrode in the electrolyte-filled cell was pressed against (resting on) the calcium fluoride IR window with the electrode adjusted to a static potential of –900 mV(AgCl/Ag). Further spectra acquired at potentials more positive than this value and ratioed versus this background were acquired to provide a series of spectra as a function of voltage. Additionally the practice of acquiring electrochemical current measurements during the IR spectral acquisition at each potential[5] was carried out to provide effectively a "single sweep voltammogram" over the timescale of the experiment.

IR spectra of model solutions prepared in DMSO and DMF consisting of mixtures of $KAuBr_4$ and the respective pseudohalide salts at various $KAuBr_4$:pseudohalide salt mole ratios (1:1, 1:2 and 1:4) were also acquired using a Press-Lok cell containing calcium fluoride windows. Scanning conditions on the Perkin Elmer Spotlight 200 FTIR spectrometer used for the transmission IR spectra were identical to what has been described previously.

ESI-MS spectra were acquired on a Bruker Electrospray Ionisation Time-of-Flight (ESI-TOF) mass spectrometer in negative ion mode of model solutions and other solutions prepared for the purpose of confirming the identity of species detected in the electrochemical cells. Samples for analysis were prepared by adding a drop of model solution (1 μL) to 1 mL of methanol to a small capped plastic vial and vortexed for 10 seconds to allow thorough mixing. This mixture was then injected via hypodermic syringe into the instrument. The parameters set on the instrument were –80.0 V for the capillary exist and 60.0 V for the hexapole RF (radio-frequency) ion guides. The skimmer voltage was –40 to –50 V and the hexapole 1 voltage in the instrument was –23.5 V. The m/z range scanned was 800.

Results and Discussion

Cyclic voltammetric studies of the Au electrode systems.— Fig. 1a to 1f illustrate the CVs of Au electrode systems in the presence of NCO^- (0.025 mol L^{-1}), NCS^-(0.05 mol L^{-1}) and $NCSe^-$(0.05 mol L^{-1}) ions co-dissolved in DMSO and DMF solvents with 0.1 mol L^{-1} TBAP as a supporting electrolyte. The CVs for all three pseudohalide ions give different looking traces with most (apart from $NCSe^-$) exhibiting some commonality of appearance between CVs done in DMSO and DMF for the same ion. In the case of Au/NCO^-/DMSO or DMF systems (Fig. 1a and 1b), the CV shows a distinct broad peak at ca. 1000 mV(AgCl/Ag) which is most likely associated with Au to Au(I) electrodissolution.[26] In the Au/NCS^-/DMF system (Fig. 1c) there are two peaks observed in the CV recorded in the DMF solvent at ca. 1000 mV(AgCl/Ag) and 1500 mV(AgCl/Ag) and both could be due to the formation of Au(I) species,[26] though the literature often provides conflicting views of this. For instance, in the paper by Dickinson and Povey,[29] the potential at which Au(III) oxide is produced on an Au electrode in sulfuric acid is ca. 1.5 V(SCE) however this is for the electrode immersed in an aqueous electrolyte. In general, the later in situ IR work to be discussed did not demonstrate the detection of Au(III)-based species (see later).

The CV produced for the Au/NCS^-/DMSO system (Fig. 1c) does not demonstrate distinct peaks. The CVs for the Au/$NCSe^-$/DMSO and Au/$NCSe^-$/DMF systems (Fig. 1e and 1f) exhibit two peaks also with the CV for the Au/$NCSe^-$/DMF system showing the most well defined peaks. The difference between the CV for this system and those exhibited in Fig. 1a to 1d is that the first peak occurs at a lower potential of 550–600 mV(AgCl/Ag). Also in the Au electrode systems

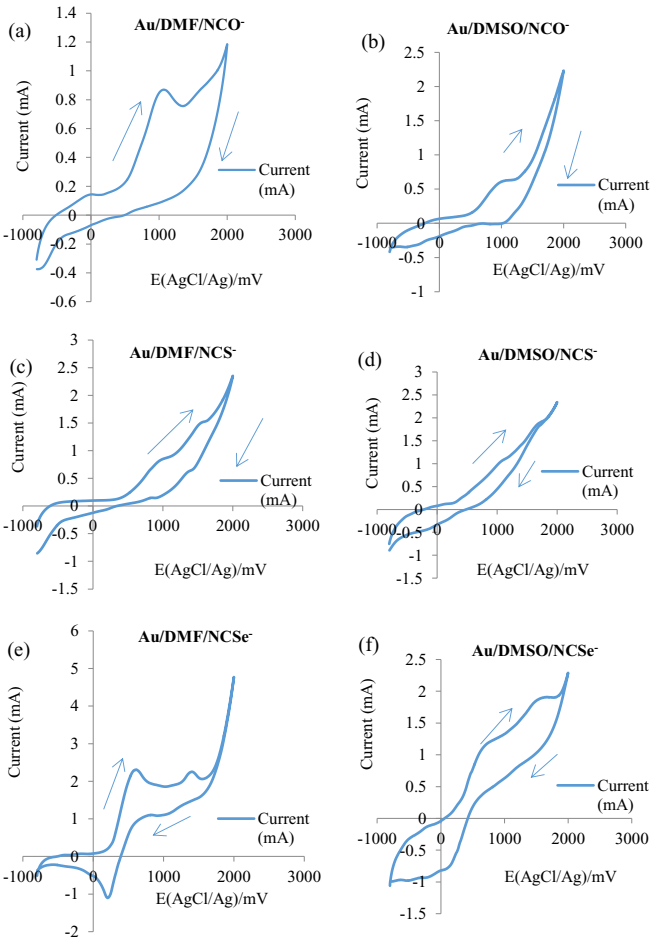

Figure 1. Cyclic voltammograms of the gold electrode in DMF and DMSO solvents containing pseudohalide ions and 0.1 mol L^{-1} TBAP (sweep rate = 20 mV/s): 0.025 mol L^{-1} KOCN in (a) DMF and (b) DMSO, 0.05 mol L^{-1} NaSCN in (a) DMF and (b) DMSO, 0.05 mol L^{-1} KSeCN in (a) DMF and (b) DMSO. Arrows show the path actually traced upon conducting the forward and backward sweep of potentials.

involving $NCSe^-$ in both DMSO and DMF, there are distinct negative-going features evident in the CVs which indicate the reduction of a deposited film on the electrode. When observing the "single sweep voltammograms" of the electrode systems (Fig S1(a) to (f) in the SI section) [acquired during the course of the SNIFTIRS experiment, see later], the appearance of the voltammograms is visibly different from the CVs illustrated in Fig. 1. This is due to the fact that the time scale of the potential at the electrode surface is different for the single sweep voltammogram from that observed for the CVs which were recorded at a sweep rate of 20 mV/s operating over a potential span of 2800 mV each way (corresponding to 4.7 minutes for the entire sweep). In contrast the single sweep voltammograms are recorded over the time scale of the SNIFTIRS experiment which averages approximately 45 minutes per run and are only for data that occur when potential is adjusted in one direction, i.e. anodically. Nevertheless in the case of the Au/NCS^- and Au/$NCSe^-$ systems, two peaks in the single sweep voltammogram can still be mostly discerned (Fig. S1(c), (e) and (f)) and almost all IR-detectable electrochemical activity in SNIFTIRS runs were invariably observed in the anodic region of the cyclic voltammograms above +200 mV (AgCl/Ag).

Martins et al.[28] have done an electrochemical study of Au dissolution kinetics in DMSO solutions of KSCN containing $LiClO_4$ as the supporting electrolyte. They state that while the faradaic processes of NCS^- ion on Pt electrodes in acetonitrile (ACN) involve

Table I. FTIR data from in situ IR spectroelectrochemical studies of Au/NCX$^-$ systems electrochemically polarized in 0.1 mol L^{-1} TBAP in DMSO or DMF solvents.

System studied	ν(CN) of free NCX$^-$ ion[5] (X = O, S, Se) cm^{-1}	ν(CN) of Au$^+$/ NCX$^-$complex ion cm^{-1}	ν(CO) of CO_2 dissolved in solvent[5] cm^{-1}	Color of cell solution after SNIFTIRS experiment
Au/DMF/NCO$^-$	2137	2230	2339	no color change
Au /DMF/NCS$^-$	2056	2123[32]	2337	no color change
Au /DMF/NCSe$^-$	2064	2125	nd	light yellow
Au /DMSO/ NCO$^-$	2136	2234	2337	no color change
Au /DMSO/NCS$^-$	2055	2124[32]	nd	no color change
Au /DMSO/NCSe$^-$	2065	2124	nd	light yellow

nd = not detected

transformations of the NCS$^-$ ion itself into various oxidation products such as $(SCN)_2$ (at lower NCS$^-$ concentrations and T < 30°C) and NCS$^-$ based polymers (at higher concentrations of NCS$^-$ and T > 30°C), the situation on Au electrodes is different. This is because the faradaic processes involve not just the ion undergoing transformations but in fact electrodissolution of the Au electrode itself to produce complex-ion species. This is supported by a later study by Benari et al.[26] although these authors make no reference to $(SCN)_2$ type by-products as Martins did.

In situ IR spectra of the Au/pseudohalide systems in DMSO and DMF.— Table I summarises all the vibrational frequencies observed in the in situ IR spectra reported for the Au/pseudohalide systems in DMSO and DMF. Further details on these assignments are provided below under each system discussed.

Au/NCO$^-$/DMSO and Au/NCO$^-$/DMF.—Fig. 2a and 2b are the SNIFTIRS spectra of the Au electrode anodically polarized in the presence of 0.025 mol L^{-1} KOCN/0.1 mol L^{-1} TBAP dissolved in DMSO and DMF respectively. Fig. 3a and 3b are the

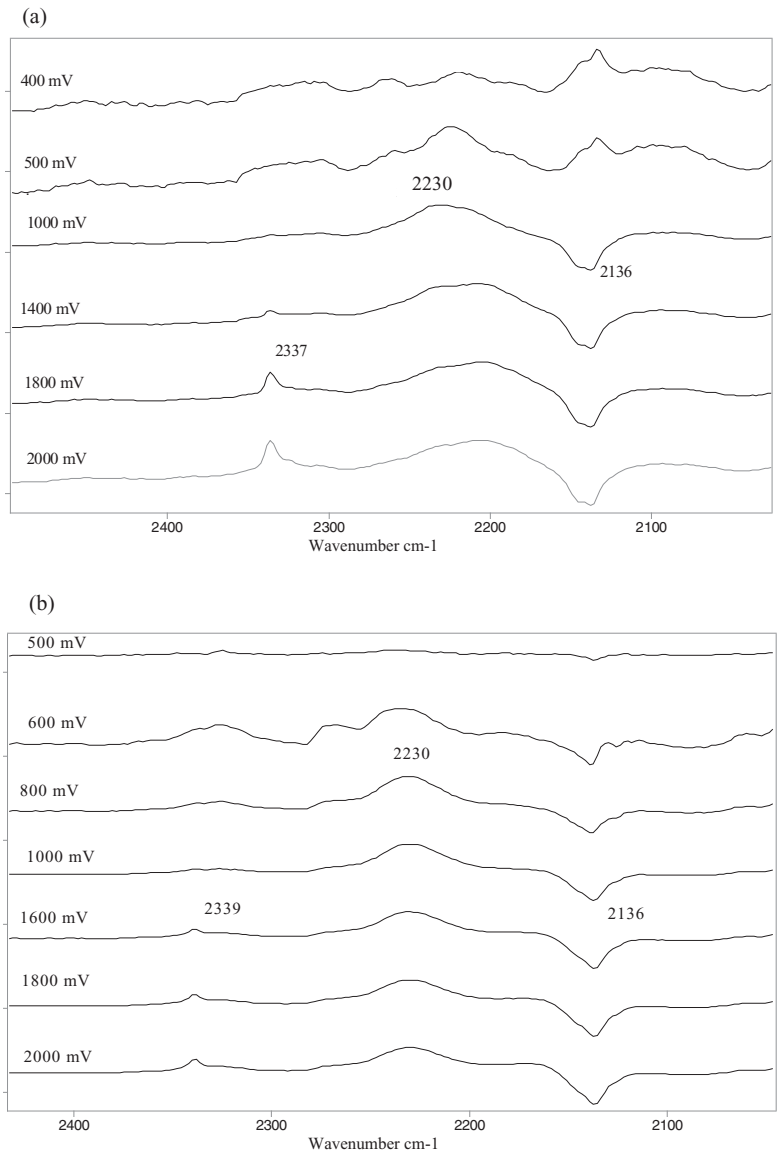

Figure 2. Series of SNIFTIRS spectra of the gold electrode as a function of applied potential in DMSO and DMF solvents containing pseudohalide ions and 0.1 mol L^{-1} TBAP. Spectra in (a) 0.025 mol L^{-1} KOCN in DMSO, (b) 0.025 mol L^{-1} KOCN in DMF.

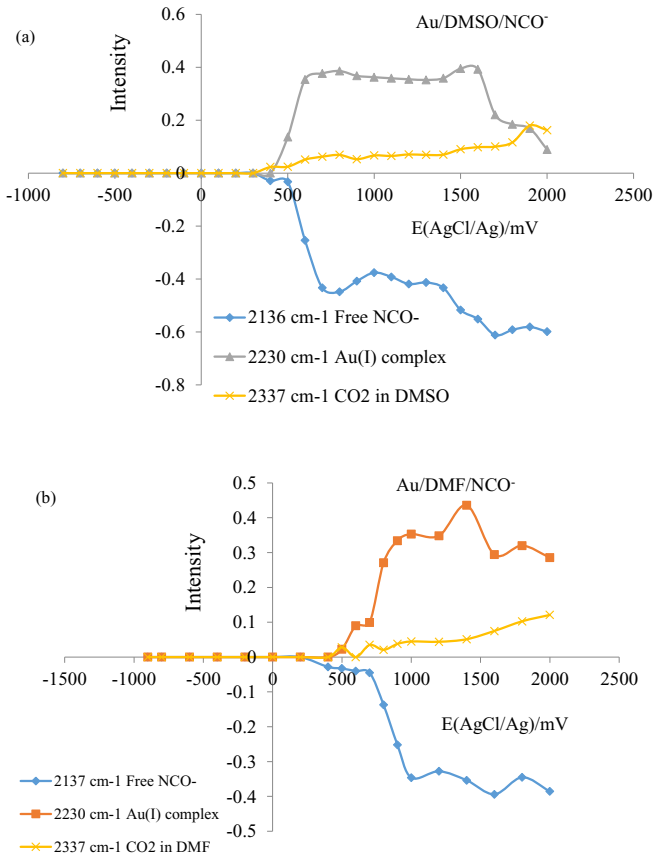

Figure 3. Plots of the intensity changes of the various molecular species generated in the thin layer during electrochemical polarization and observed in the SNIFTIRS spectra as a function of applied potential in the gold electrode as a function of applied potential in DMSO and DMF solvents containing pseudohalide ions and 0.1 mol L^{-1} TBAP. (a) 0.025 mol L^{-1} KOCN in DMSO, (b) 0.025 mol L^{-1} KOCN in DMF.

corresponding intensity/applied potential plots showing intensity changes in detected molecular species as a function of applied potential for the Au/NCO^-/DMSO and Au/NCO^-/DMF respectively. The single sweep voltammograms pertaining to these systems are illustrated in Fig S1(a) and S1(b).

Inspection of the spectra in Fig. 2a and 2b reveal three main species in this system which give peaks at 2137/2147 cm^{-1}, 2230 cm^{-1} and 2337 cm^{-1}. The characteristically double-headed peak at 2137/2147 cm^{-1} is due to free cyanate ion in DMSO and DMF electrolyte. This characteristic shape seen in DMSO and DMF is due to its being dissolved in a solvent with which it interacts less strongly and hence shows up more fine structure[30] present in the IR absorption band compared to aqueous solvents where the expectedly stronger intermolecular forces of water have caused the vibrational peaks of the cyanate ion to blend together to form a mostly symmetrical/smoother looking peak. This smoother peak has been observed in earlier SNIFTIRS studies involving aqueous electrolytes.[17,18]

The spectral behavior of the 2137/2147 cm^{-1} peak does not change until the anodic region is entered where it shows negative intensity relative to the background recorded at –900 mV(AgCl/Ag). This indicates the ion is being consumed at the Au electrode surface as it is anodically polarized to form complex ion species and undergo electro oxidation. The drop in intensity as seen in Fig. 3a and 3b is sharp over the region 700–1000 mV(AgCl/Ag) for the Au electrode in DMF and over the 500–700 mV(AgCl/Ag) region for DMSO before it levels off. Paralleling this decrease in intensity of the 2137/2147 cm^{-1} peak in Figs. 3a and 3b is an increase in the intensity of the broad 2230 cm^{-1} peak. The origin of peaks observed in this region of the spectrum has been subject to various interpretations. One study by Zhen et al.[25] states that a weak, broad peak was observed at 2230 cm^{-1} in their in situ IR spectra of a Au(III) single crystal electrode (adjusted to 0.5 V (SCE)) in the presence of 0.1 mol L^{-1} NaOH and 50 mmol L^{-1} glycine. This was interestingly assigned to an insoluble AuCN film. However, in the present study involving polar aprotic solvents, it is believed that this peak is due to a Au(I) complex ion species forming through electrodissolution of the Au to Au(I) and subsequent complexation with cyanate ion to form a species thought to be $[Au(NCO)_2]^-$. Although no study has reported the IR stretching frequency of this simple ion in DMSO, DMF or even aqueous solution, the CN stretching frequency is close in magnitude to the 2251 cm^{-1} CN stretching frequency detected in the KBr disk IR spectrum of solid $[Ph_4As]Au(NCO)_2$ as reported by Beck et al.[31] Model solution work reported later in this paper also supports the assignment of this species to the $[Au(NCO)_2]^-$ ion. The observation of this species hence supports the views of Benari et al. and Martins et al[26,28] that the Au is undergoing active dissolution in this region to form Au(I) complex ion species. The intensity of this peak as a function of applied potential at the Au electrode increases sharply as stated earlier but then levels off which could indicate the deposition of an insoluble film on the electrode surface containing the Au(I) species. This may have occurred due to large onset of formation of Au(I) at the electrode followed by complexation, increase in concentration and then precipitation due to saturation of the thin layer with this compound. The other peak observed in SNIFTIRS spectra (Fig. 2a, 2b) is a peak at 2337 cm^{-1} which based on earlier work published[5] can be assigned to electrogenerated CO_2 dissolved in the DMSO or DMF solvent. The source of this CO_2 is likely to be from the oxidation of cyanate ion or solvent oxidation. Its intensity as a function of applied potential (Fig. 3a and 3b) is low with a slight increase being observed as more anodic potentials are applied at the Au electrode. The difference in electrochemical behavior between the DMSO and DMF solvents was small. Apart from the region corresponding to the sharp drop in free cyanate ion intensity in SNIFTIRS spectra, DMSO and DMF generally exhibit almost identical behavior in terms of speciation observed at the electrode surface.

Au/NCS^-/DMSO and Au/NCS^-/DMF.—Fig. 4a and 4b are the SNIFTIRS spectra of the Au electrode anodically polarized in the presence of 0.05 mol L^{-1} NaSCN/0.1 mol L^{-1} TBAP dissolved in DMSO and DMF respectively. The higher concentration of NCS^- used in this experiment was due to the greater solubility of this salt in the electrolyte relative to KOCN which remained partially undissolved at the same concentration. Fig. 5a and 5b are the corresponding intensity/applied potential plots showing intensity changes in detected molecular species as a function of applied potential for the Au/NCS^-/DMSO and Au/NCS^-/DMF respectively. The single sweep voltammograms pertaining to these systems are illustrated in Fig S1(c) and S1(d).

Inspection of the spectra in Fig. 4a and 4b reveal two main species in this system (as well as a third minor one) all of which give peaks at 2055 cm^{-1}, 2123 cm^{-1} and 2337 cm^{-1}.

The spectral behavior of the 2055 cm^{-1} peak (similar to the NCO^- system) attributed to free thiocyanate ion does not change or even register a peak until the anodic region is entered where it shows negative intensity relative to the background recorded at –900 mV(AgCl/Ag). This indicates, as in the Au/NCO^- system case that the free thiocyanate ion is being consumed at the Au electrode surface as it undergoes anodic dissolution to form complex ion species and also when the NCS^- ion undergoes electro oxidation itself at the electrode (the products of which are not immediately observed in the CN stretching region). The drop in intensity as seen in Fig. 5a and 5b is very sharp over the region 700–900 mV(AgCl/Ag) for the Au electrode in DMSO and over the 600–800 mV(AgCl/Ag) region for DMF before it fluctuates/levels off. Paralleling this decrease in intensity of the 2055 cm^{-1} peak in Fig. 5a and 5b is an increase in the intensity of the broad 2123 cm^{-1} peak. This peak can be unequivocally attributed to an Au(I) complex ion species with NCS^- ion, i.e. $[Au(SCN)_2]^-$.

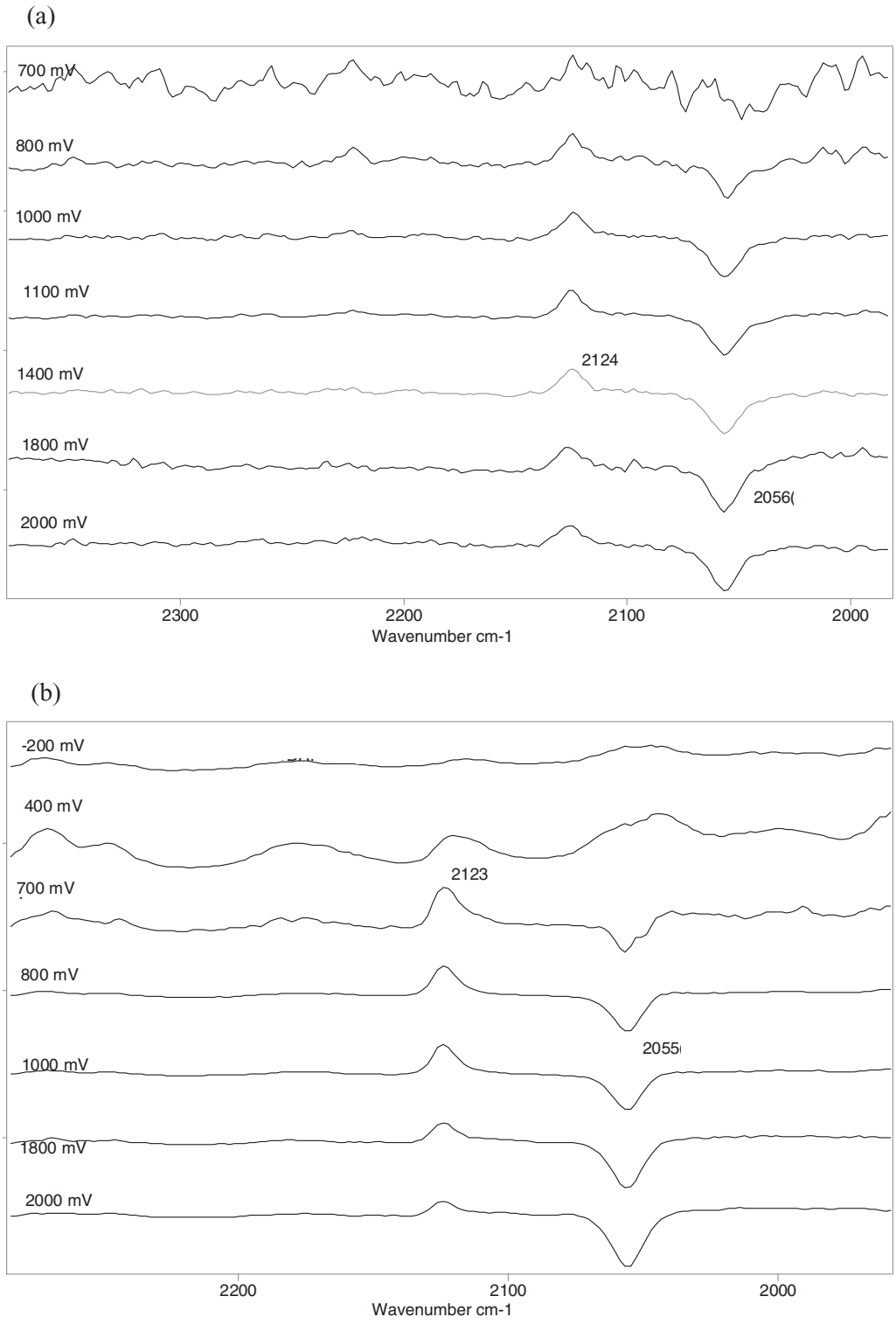

Figure 4. Series of SNIFTIRS spectra of the gold electrode as a function of applied potential in DMSO and DMF solvents containing pseudohalide ions and 0.1 mol L^{-1} TBAP. (a) 0.05 mol L^{-1} NaSCN in DMSO, (b) 0.05 mol L^{-1} NaSCN in DMF.

This is well supported by literature studies[32,33] in which the CN stretching frequency of this has been determined for this complex ion in non-aqueous media. For instance, Bowmaker and Rogers[32] reported that a peak observed at 2120 cm^{-1} in a dichloromethane solution of $[NBu_4]Au(SCN)_2$ was due to the $[Au(SCN)_2]^-$ ion in solution. In the same study, it is also shown that Au bonds to S in this complex and not N as would be the case with $[Au(NCO)_2]^-$ discussed earlier. Hence it is obvious that at 500–600 mV (AgCl/Ag), Au dissolves to form Au(I) which then is complexed by NCS^- ion to form $[Au(SCN)_2]^-$. Fig. 5a and 5b, show a levelling off of the intensity of 2123 cm^{-1} peak at about 1000 mV(AgCl/Ag) which may be indicative of an insoluble film of the complex ion forming on the electrode surface due to the burst of formation of the Au(I) complex and its release into the thin layer so saturating the solution. There is a distinct peak observed

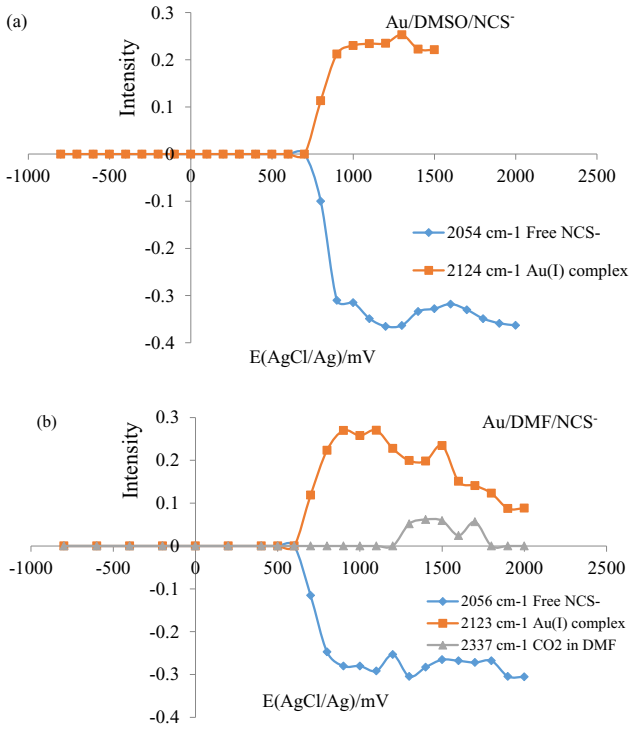

Figure 5. Plots of the intensity changes of the various molecular species generated in the thin layer during electrochemical polarization and observed in the SNIFTIRS spectra as a function of applied potential in the gold electrode as a function of applied potential in DMSO and DMF solvents containing pseudohalide ions and 0.1 mol L^{-1} TBAP. (a) 0.05 mol L^{-1} NaSCN in DMSO, (b) 0.05 mol L^{-1} NaSCN in DMF.

in the single sweep voltammogram of the Au/NCS^-/DMF system at ca. 700 mV(AgCl/Ag) (Fig. S1(c)) which can be clearly associated with the Au to Au(I) electrodissolution event. An additional peak just before +1500 mV(AgCl/Ag) could be a Au to Au(III) oxidation peak but it does not appear to be associated with the emergence in the IR of any $[Au(SCN)_4]^-$ species which has been reported to be isolated as an unstable insoluble red solid from cold aqueous reaction mixtures of Au(III) and thiocyanate ion.[34] In the present study, the cell solution was observed to remain colorless during this in situ IR experiment so suggesting that this complex ion species has not formed. Furthermore, the IR spectrum did not reveal any new peaks other than those discussed above which might be associated with this species.

The other peak observed in SNIFTIRS spectra is a peak at 2337 cm^{-1} which can be assigned to electrogenerated CO_2. This was only observed in the DMF solvent. The source of this CO_2 is likely to be from the oxidation of DMF. This is supported by the fact that it is only observed as a minor species at 1200–1500 mV(AgCl/Ag) where DMF would be expected to become oxidised at the electrode surface.[5]

Au/$NCSe^-$/DMSO and Au/$NCSe^-$/DMF.—Fig. 6a and 6b are the SNIFTIRS spectra of the Au electrode anodically polarized in the presence of 0.05 mol L^{-1} KSeCN/0.1 mol L^{-1} TBAP dissolved in DMSO and DMF respectively. The higher concentration of $SeCN^-$ used in this experiment was due to the greater solubility (in common with NaSCN) of this salt in the electrolyte. Fig. 7a and 7b are the corresponding intensity/applied potential plots showing intensity changes in detected molecular species as a function of applied potential for the Au/$NCSe^-$/DMSO and Au/$NCSe^-$/DMF respectively. The single sweep voltammograms pertaining to these systems are illustrated in Fig S1(e) and S1(f).

Inspection of the in situ IR spectra in Fig. 6a and 6b reveals two main species in this system which give peaks at 2065 cm^{-1} and 2124–2126 cm^{-1}.

The 2065 cm^{-1} peak can be attributed to free selenocyanate ion dissolved in the polar aprotic solvent. This agrees with the vibrational frequency reported for KSeCN dissolved in butanone solution[35] and has a lower vibrational frequency compared to that observed for the ion dissolved in water[18] as expected for this lower polarity solvent. In common with the Au/NCS^- and Au/$NCSe^-$ systems, the free ion peak does not appear in the IR spectrum until the anodic region is entered where it shows negative intensity relative to the background recorded at –900 mV(AgCl/Ag). This indicates, as in the other systems that the free selenocyanate ion is being consumed at the Au surface as the electrode undergoes anodic dissolution to form complex ion species and also when the $NCSe^-$ ion, itself, undergoes electro-oxidation at the electrode (the products of which are not immediately observed in the CN stretching region). When observing the intensity vs applied potential plots in Fig. 7a and 7b, sharp/sudden increases/decreases in the intensities of the peaks due to the free ion and the peak at 2124–2126 cm^{-1} followed by a drop and levelling off of the intensities indicates an anodic dissolution event where Au is oxidised to Au(I) after 500 mV(AgCl/Ag) and then probably forms an adherent film on the surface of the electrode. This is supported also by the single sweep voltammograms (Fig. S1(e) and (f)) which show a plateau of current after 500 mV(AgCl/Ag). This lasts until 1600 mV(AgCl/Ag) after which the current increases sharply due most likely to events like oxidation of the solvent (DMSO or DMF). Furthermore, after the in situ IR experiment, a black film was observed on the Au electrode surface.

The drop in the intensity to more negative values of the 2065 cm^{-1} free selenocyanate ion peak is paralleled by an increase in intensity of the peak at 2124–2126 cm^{-1}. As in the Au/NCS^- system, this peak can be unequivocally attributed to an Au(I) complex ion species with $NCSe^-$ ion. It is strongly believed this is due to the $[Au(SeCN)_2]^-$ ion dissolved in DMSO or DMF. While direct spectroscopic evidence does not appear to exist in the literature for this ion, it can be inferred to be the case from the similarity of its vibrational frequency to that of the $[Au(SCN)_2]^-$ ion as detected in the Au/NCS^- electrochemical system discussed previously.

The in situ IR results suggest mechanistically that the formation of all the Au(I) complex ions in the Au/pseudohalide ion/DMSO or DMF systems at the electrode surface involve the one electron oxidation of elemental Au to Au(I) and its combination with the relevant pseudohalide ion to form the complex ion. Martins et al.[27] concluded that the kinetics of gold dissolution in NaSCN-containing acetonitrile electrolytes were similar to those of gold electrodes in aqueous electrolytes containing complexing ions. They considered that the dissolution proceeds via a surface intermediate consisting of adsorbed NCS^- on Au which leads eventually to oxidation of Au and formation of $[Au(SCN)_2]^-$ via the reaction

$$Au + 2SCN^- \rightarrow [Au(SCN)_2]^- + e^-$$

It is thus implied on the basis of the in situ IR results obtained in this study that a similar mechanism of anodic dissolution is operating in the Au electrode systems containing the DMSO and DMF solutions of NCO^-, NCS^- and $NCSe^-$.

Model Solution work for verifying species observed in in situ IR spectra.— In order to provide a verification of the species observed in the in situ IR spectra provided of the Au/NCO^-, Au/NCS^- and Au/$NCSe^-$ systems as discussed above, model solution work was carried out in order to make species detected in in situ IR spectra independently of their electrochemical method of generation in order to prove the identity of them. This involved the mixing of DMSO/DMF solutions of $KAuBr_4$ and the pseudohalide salts (NCO^-, NCS^- and $NCSe^-$) in 1:1 and 1:2 mole ratios for solutions made in DMF (due to solubility issues of the salts in this solvent) and 1:1, 1:2 and 1:4 mole ratio solutions for solutions made in DMSO (in which the solubilities of the pseudohalide salts were better than in DMF). These model solutions were then examined using transmission IR spectra of a thin layer of the solutions created between calcium fluoride windows as previously described.[5]

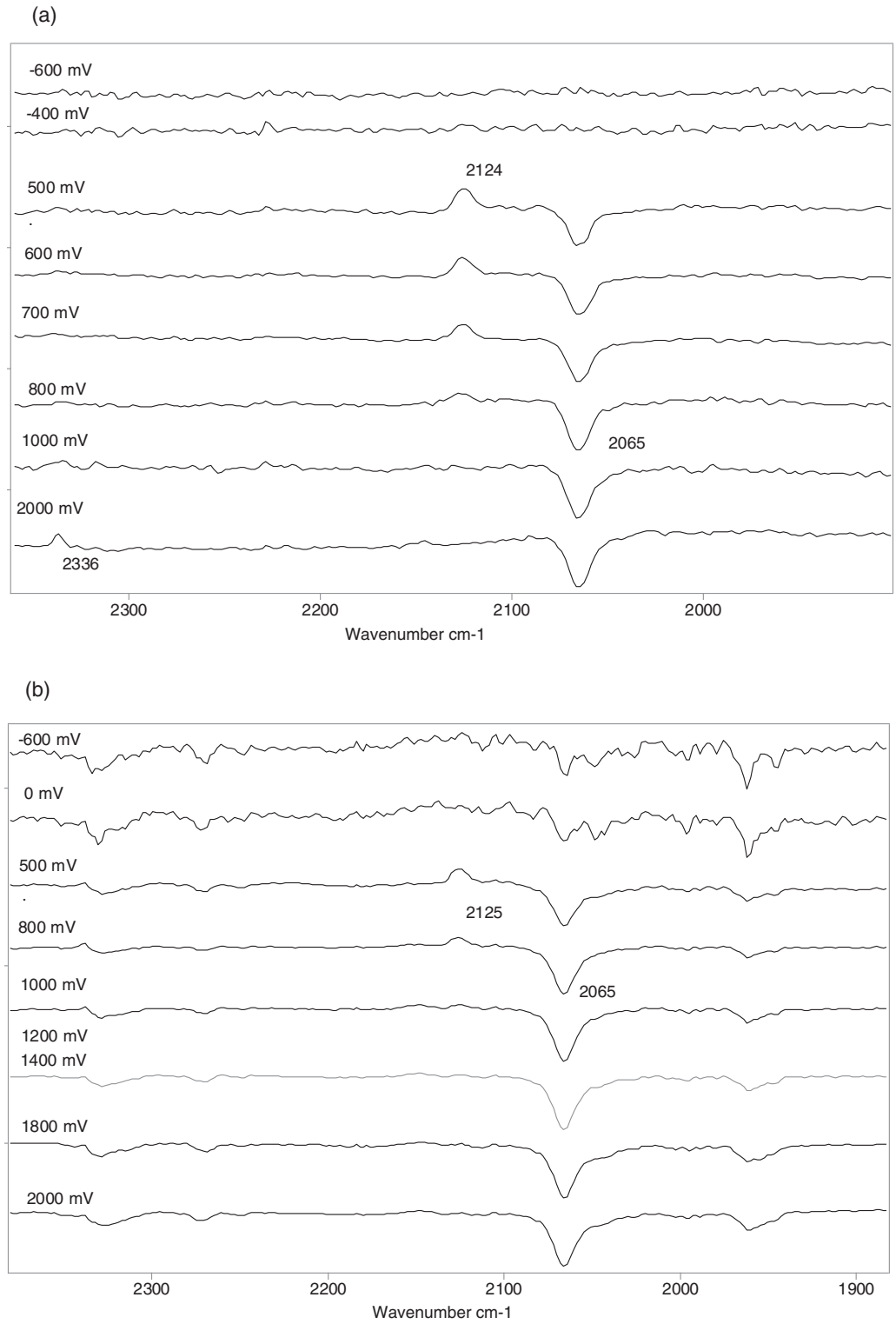

Figure 6. Series of SNIFTIRS spectra of the gold electrode as a function of applied potential in DMSO and DMF solvents containing pseudohalide ions and 0.1 mol L^{-1} TBAP. (a) 0.05 mol L^{-1} KSeCN in DMSO, (b) 0.05 mol L^{-1} KSeCN in DMF.

Table II is a summary of the IR data collected from the model solution spectra.

$KAuBr_4$/KOCN model solutions.—As is evident in Table II, the IR spectra show a peak ranging from 2163–2168 cm^{-1} in the two solvents. No peak due to the free cyanate ion was observed apart from the $KAuBr_4$:KOCN 1:4 mole ratio solution where a small shoulder at 2136 cm^{-1} was observed on the more intense peak at ca. 2163 cm^{-1}. The wavenumber value at 2163–2168 cm^{-1} is obviously not the same as the wavenumber value observed in the in situ IR spectra of the Au/NCO^- electrochemical system which was at 2230 cm^{-1}. This is because in the model solutions consisting of $KAuBr_4$ and KOCN, another species different to that observed in the electrochemical experiments has formed, and this species is a Au(III)-cyanate complex or complexes. To test this, it was decided to carry out an ESI-MS

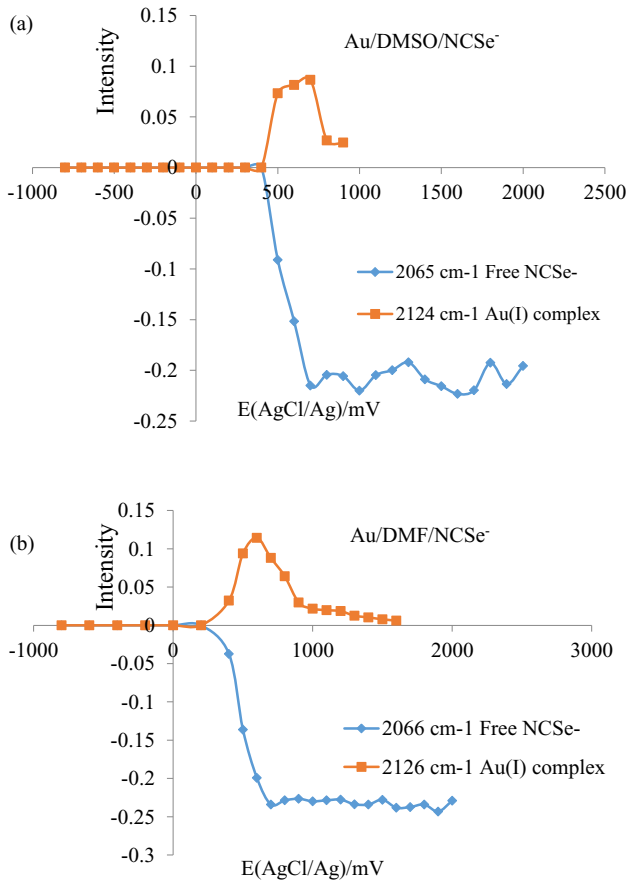

Figure 7. Plots of the intensity changes of the various molecular species generated in the thin layer during electrochemical polarization and observed in the SNIFTIRS spectra as a function of applied potential in the gold electrode as a function of applied potential in DMSO and DMF solvents containing pseudohalide ions and 0.1 mol L^{-1} TBAP. (a) 0.05 mol L^{-1} KSeCN in DMSO, (b) 0.05 mol L^{-1} KSeCN in DMF.

spectrum of the 1:4 mole ratio (Au(III):NCO^-) model solution to gain an idea of what species are likely to be present in the actual solution. Fig. 8a illustrates the ESI-MS spectrum of this sample diluted in methanol before introducing it into the ESI-MS instrument. The spectrum is dominated by an intense peak at m/z = 364.97 which can be assigned to the species $[Au(NCO)_4]^-$, a gold(III) complex ion. This agrees with the expected isotopic splitting of the peak which will only show weak splitting due to ^{13}C which gives a weak peak at m/z = ~366. In addition there are other peaks which are much weaker than the m/z = 364.97 peak. These species are easy to identify due to the more significant isotopic patterns produced by the Br^- ion which is present in these complexes. Table III is a summary of the assignments made for this system and others to be discussed. Hence characteristic peaks at m/z 401.90 and 440.82 are observed which are assigned to $[Au(NCO)_3Br]^-$ and $[Au(NCO)_2Br_2]^-$ respectively. Another weak peak is also observed at m/z = 280.98. This is believed to be due to the species $[Au(NCO)_2]^-$ which is not likely to be present in the solution but has occurred as an artifact as a result of reduction arising out of the use of a negative cone voltage in the ESI-MS experiment.[36] The ESI-MS work hence confirms that the peaks observed at 2162–2168 cm^{-1} in the IR spectra (in both DMF and DMSO) of the $KAuBr_4$/KOCN model solutions are due to Au(III)-cyanate complexes. Literature with IR data for discrete simple Au(III)-NCO complexes to support this assignment appears, however, to be lacking hence this work reports this for the first time. In DMSO solutions, there is a small shift of the ν(CN) stretching frequency in going from 1:1 to 1:4 $KAuBr_4$:KOCN mole ratio solutions which indicates the formation of higher order complexes such as $[Au(NCO)_4]^-$. It remains however to prove that $[Au(NCO)_2]^-$ can be synthesized in solution independently of the electrochemical cell. This was provided in later experiments where the Au(III) starting salt was reduced initially to Au(I) by premixing with NaSCN (see later).

$KAuBr_4$/NaSCN model solutions.—Table II shows that when mixing $KAuBr_4$ and NaSCN in different mole ratios (varying from 1:1 to 1:4 $KAuBr_4$:NaSCN) three peaks were generally observed in the IR spectra. These peaks occurred at 2055, 2120.5 and 2143 cm^{-1}. The peak at 2055 cm^{-1} is due to the free NCS^- ion as expected. The other weak peak at 2120.5 cm^{-1} can be assigned to $[Au(SCN)_2]^-$ ion although it is 3–4 cm^{-1} different from the peak observed in the in situ IR experiment (see Table I). This result from the model solution IR

Table II. FTIR data from IR studies of DMF or DMSO model solutions of $KAuBr_4$ and potassium (or sodium) pseudohalide ion salts prepared with different mole ratios.

Model solution studied and mole ratio of $KAuBr_4$: pseudohalide salt prepared in DMF or DMSO (X = O, S, Se)	ν(CN) of free NCX^- ion[5] (X = O, S, Se) cm^{-1}	ν(CN) of Au(I)/Au(III)/NCX^-complex ion cm^{-1}	Observed color of solution
DMF			
$AuBr_4$/ KOCN 1:1	nd	2168 s	Blood red
$AuBr_4$/ KOCN 1:2	nd	2168 s	
$AuBr_4$/ NaSCN 1:1	nd	nd	Blood red
$AuBr_4$/ NaSCN 1:2	2055	2120[32] w	
$AuBr_4$/ KSeCN 1:1	nd	nd	Orange/yellow
$AuBr_4$/ KSeCN 1:2	2065	2126 w	Yellow
DMSO			
$AuBr_4$/ KOCN 1:1	nd	2166	Blood red
$AuBr_4$/ KOCN 1:2	nd	2165	
$AuBr_4$/ KOCN 1:4	2136	2165	
$AuBr_4$/ NaSCN 1:1	2055 w	nd	Blood red
$AuBr_4$/ NaSCN 1:2	2055	2120[32]	
$AuBr_4$/ NaSCN 1:4	2055	2120, 2143[38] w	
$AuBr_4$/ KSeCN 1:1	nd	nd	
$AuBr_4$/ KSeCN 1:2	2065	2124	Orange/yellow
$AuBr_4$/ KSeCN 1:4	2065	2124, 2143[38] w	Yellow

nd = not detected, s = strong, w = weak

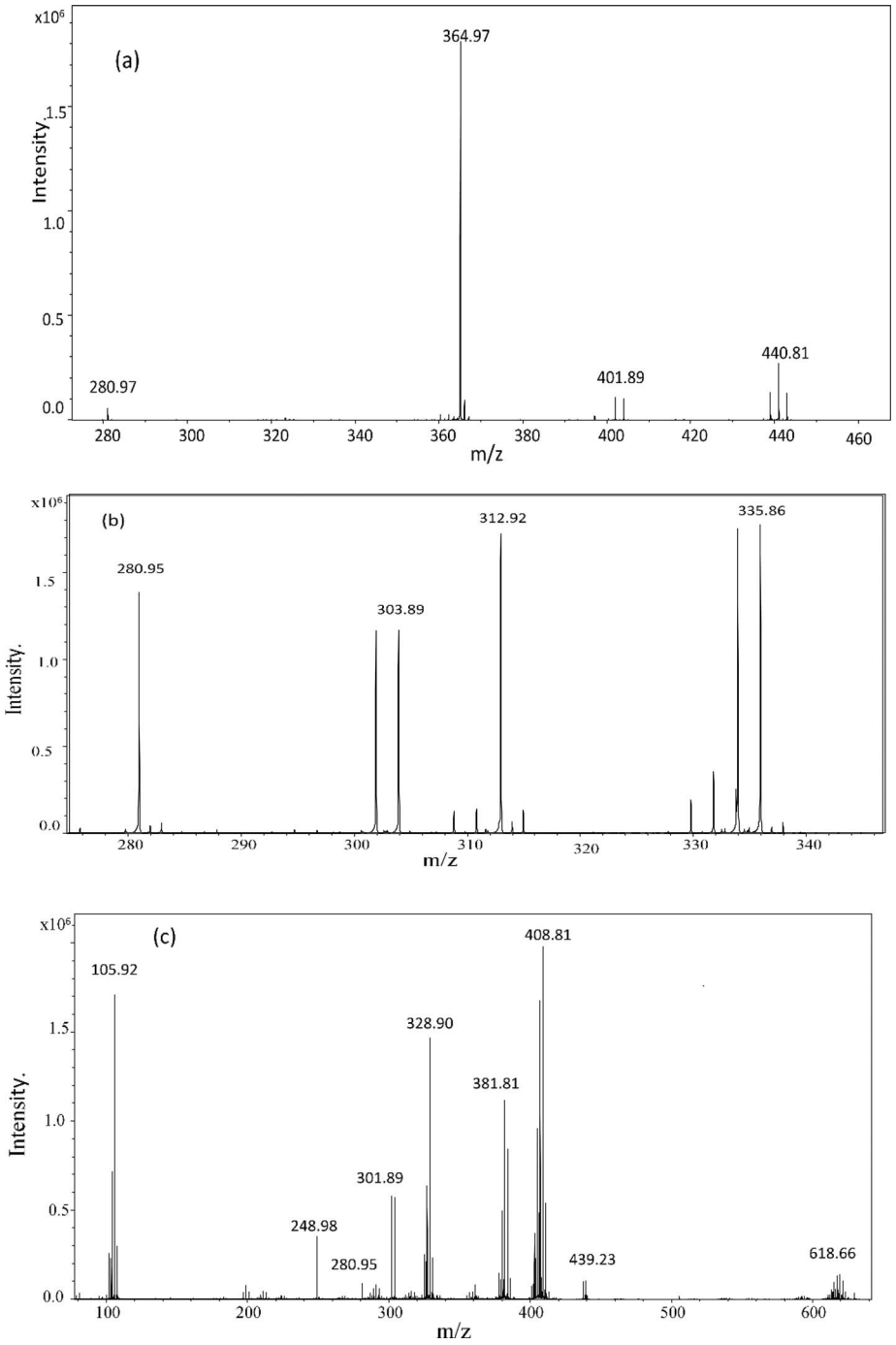

Figure 8. Electrospray ionisation mass spectra (ESI-MS) of the Au(III) pseudohalide complexes in the model solutions prepared with $KAuBr_4$ salts and pseudohalide salts in DMSO solution where $[KAuBr_4] = 0.025$ mol L^{-1} and [pseudohalide salt] = 0.1 mol L^{-1}. The sample was diluted in methanol before introducing into the ESI-MS by adding a drop of model solution (1 μL) to 1 mL of methanol. (a) 1:4 $KAuBr_4$:KOCN mole ratio solutions, (b) 1:4 $KAuBr_4$:NaSCN mole ratio solutions, (c) 1:4 $KAuBr_4$:KSeCN mole ratio solutions.

Table III. Electrospray mass data of the species observed in the model solutions prepared with $KAuBr_4$ salts and pseudohalide salts which are present in a $KAuBr_4$:pseudohalide salt 1:4 mole ratio in DMSO solution. (Mass (m/z) values are rounded to whole numbers).

$KAuBr_4$/KOCN model solutions		$KAuBr_4$/NaSCN model solutions		$KAuBr_4$/KSeCN model solutions	
Au(III) complexes	Mass (m/z)	Au(I) complexes	Mass (m/z)	Au(I)/Au(III) complexes	Mass (m/z)
$[Au(NCO)_2Br_2]^-$	441	$[Au(SCN)_2]^-$	313	$SeCN^-$	106
$[Au(NCO)_3Br]^-$	402	$[Au(SCN)Br]^-$	336	$[Au(SeCN)_2]$-	409
$[Au(NCO)_4]^-$	365	$[Au(CN)Br]^-$	304	$[Au(SeCN)Br]^-$	382
		$[Au(SCN)(CN)]^-$ and $[Au(NCO)_2]^-$	281	$[Au(SeCN)_4]^-$	619
		*$[Au(NCO)(CN)]^-$	265	$[Au(SeCN)CN]^-$	329

*This is a mixed solution containing $KAuBr_4$, NaSCN and KOCN in a 1:4:4 $KAuBr_4$: NCS^- : NCO^- mole ratio.

experiments proves that NCS^- ion is reducing the Au(III) present in $KAuBr_4$ to Au(I) which subsequently forms a complex with NCS^- ion in solution to generate the complex ion, $[Au(SCN)_2]^-$. This was confirmed by recording the ESI-MS spectrum of the 1:4 $KAuBr_4$: NaSCN model solution in DMSO which is shown in Fig. 8b. This featured a group of 4 major peaks at m/z 280.95, 303.90, 312.93 and 335.87 which can be assigned to $[Au(SCN)(CN)]^-$, $[Au(CN)Br]^-$, $[Au(SCN)_2]^-$ and $[Au(SCN)Br]^-$. All of these species are Au(I) species which reflects that redox reactions have occurred in this solution reducing Au(III) to Au(I). This agrees with previous literature on the subject.[37] Of note is the m/z peak at 312.9 due to the stable $[Au(SCN)_2]^-$ ion which is proof the ion exists in the model solution. It is interesting to note that the other species are mixed ligand species with one involving Br^- and CN^- ion. The detection of a Au-cyano species suggests that the NCS^- ion itself has been induced to convert to CN^- due to the strong thermodynamic driving force of forming a Au(I) cyano complex ion. This would explain the peak observed at 2143 cm^{-1} which on the basis of its similarity to the vibrational frequency of $[Au(CN)_2]^-$ in solution is probably due to a C-N stretch of a coordinated cyanide group bound to a Au(I) center.[38] Conversion of NCS^- to CN^- is known[37,39] to occur in acidic aqueous solution via thiocyanous acid formation. In DMSO, however, NCS^- is more stable as an ion,[40] however mixing Au(III) with thiocyanate ion leads to a redox reaction as discussed above producing Au(I) species which may induce side reactions in which the NCS^- is converted to CN^-. The driving force for such a reaction is the stability of the resultant Au-CN-type complex ion formed in solution. This is because the $[Au(CN)_2]^-$ ion is reported to have one of the highest formation constants known for a transition metal complex ion with K values[41] in the vicinity of 10^{37} L^2 mol^{-2}.

$KAuBr_4$/KSeCN model solutions.—In common with the $KAuBr_4$/NaSCN model solution systems, the IR spectra of the KSeCN based model solutions also feature three peaks which occur at 2065, 2124 and 2143 cm^{-1}. On the basis of assignments provided for the $KAuBr_4$/NaSCN model solution discussed above, these peaks may be assigned to free selenocyanate ion (2065 cm^{-1}), the $[Au(SeCN)_2]^-$ complex ion (2124 cm^{-1}) and a gold-cyano complex (2143 cm^{-1}) respectively. The wavenumber value of the peak assigned to $[Au(SeCN)_2]^-$ is identical to that observed in the in situ IR spectra of the Au/$NCSe^-$ electrochemical system (compare Table I and II, and Fig. 6). The ESI-MS spectrum for the 1:4 mole ratio $KAuBr_4$/KSeCN model solution in DMSO is shown in Fig. 8c.

In systems involving Se-containing species, the distinct isotopic splitting patterns produced by the natural isotopes of selenium facilitate identification of species as the Se atom has 6 stable isotopes.[42] The ESI-MS spectra hence predictably gave very rich isotopic splitting patterns which could be easily matched by simulation and ascribed to Se-containing species (see Table III). For example, free $NCSe^-$ ion gave a characteristic pattern of peaks centered at m/z 105.9. In addition, there was a peak assignable to $[Au(SeCN)_2]^-$ (m/z = 408.8) which confirmed the existence of this ion in solution as intimated by the IR spectra. This confirmed that a redox process had occurred also in this model solution where Au(III) had become reduced to Au(I). There was also evidence of a weak peak due to the Au(III)-selenocyanate complex, i.e. $[Au(SeCN)_4]^-$ at m/z 618.66. In addition there was evidence of other complex ion species (also noticed in the $KAuBr_4$/NaSCN DMSO model solution ESI-MS spectra), which involved the Br^-, $NCSe^-$ and CN^- ions. These species occurred at m/z 381.8 ($[Au(SeCN)Br]^-$), m/z 328.9 ($[Au(CN)(SeCN)]^-$), m/z 301.9 ($[Au(CN)Br]^-$) and m/z 248.9 ($[Au(CN)_2]^-$). All of these ions involved Au in the +1 oxidation state with the Au(I)-cyano species being of particular note as the presence of these confirmed that $NCSe^-$ had also undergone chemical conversion to CN^- as had happened in the $KAuBr_4$/NaSCN model solution in DMSO. The detection of a peak at 2143 cm^{-1} in the IR spectrum of the 1:4 mole ratio $KAuBr_4$/KSeCN model solution in DMSO is IR proof of the existence of these Au(I) cyano complexes in solution.

Further experiments to prove the existence of $[Au(NCO)_2]^-$ ion through the use of model solutions.—Earlier it was shown that the mixing of $KAuBr_4$ with KOCN in DMSO in 1:1, 1:2 and 1:4 mole ratio solutions (with respect to $KAuBr_4$:KOCN) did not lead to the formation of a Au(I) complex ion as evidenced by the different ν(CN) stretching frequencies observed in the FTIR transmission spectrum of the model solution. Instead Au(III) –cyanate complexes were formed. In order to use model solutions to prove that the complex ion $[Au(NCO)_2]^-$ suggested to form during the anodic dissolution of Au in cyanate-containing DMSO (and DMF) solutions (see Fig. 2), could be formed independently, a strategy exploiting the redox chemistry described above for the Au/NCS^- and Au/$NCSe^-$ model solution systems had to be used. It is known that in $KAuBr_4$/NaSCN model solutions, a redox reaction occurs to produce Au(I)) complexes in solution. To exploit this reaction to generate the $[Au(NCO)_2]^-$ ion, "flooding" of an initially mixed $KAuBr_4$/NCS^- model solution preparation was done in order to form a complex of $[Au(NCO)_2]^-$ by displacement of the existing NCS^- ion from $[Au(SCN)_2]^-$ ions present. Upon doing this experiment and running the IR spectra, the strategy appeared to work as is shown in Fig. 9a–9d which illustrate a series of IR spectra of $KAuBr_4$/NaSCN and $KAuBr_4$/NaSCN/KOCN solutions where the latter ("cyanate-flooded") system is studied as a function of $KAuBr_4$:KOCN mole ratio (varying from 1:1 to 1:4) with the $KAuBr_4$:NaSCN mole ratio kept constant at 1:4.

In Fig. 9a, 3 peaks are observed at 2055.4, 2120.5 and 2143 cm^{-1}. As indicated in Table II, the peaks detected in the IR spectrum are due to the free thiocyanate ion at 2055.4 cm^{-1} with the two weaker peaks being to complex ion species $[Au(SCN)_2]^-$ (2120.5 cm^{-1}) and the putative Au-cyano complex (2143 cm^{-1}) as discussed above.

In Fig. 9b to 9d, the spectra presented represent model solutions where relatively more cyanate ion has been added to the $KAuBr_4$/NaSCN model solutions. In Fig. 9c and 9d the consequences of the cyanate addition to the solution was to cause the appearance of an additional broad peak at 2246 cm^{-1} (Fig. 9c) which shifted to 2234 cm^{-1} in Fig. 9d. An additional asymmetrical peak was also observed at 2147.5 cm^{-1} in Fig. 9d corresponding to the solution with the greatest amount of cyanate ion added. These extra peaks can be readily assigned to cyanate-containing species. The peak at 2147.5 cm^{-1} observed in Fig. 9d is due to the free cyanate ion and has the typical peak shape expected for this ion when it is dissolved in

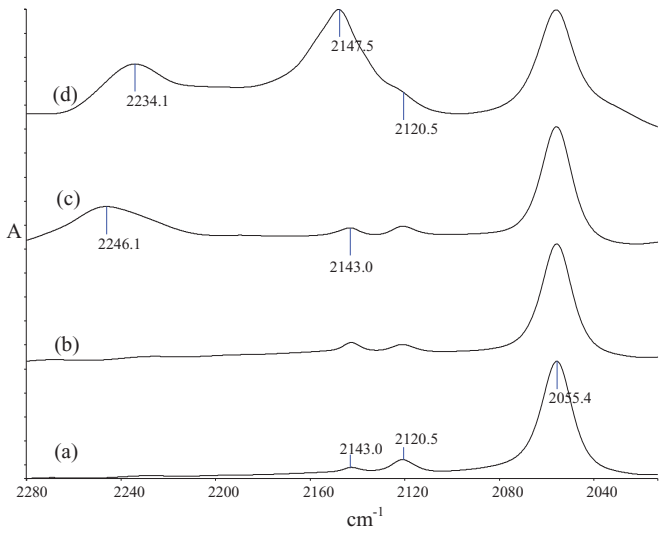

Figure 9. Transmission IR spectra of the model solutions prepared with $KAuBr_4$ salts and pseudohalide salts in DMSO solution where $KAuBr_4$ = 0.025 mol L^{-1}, NaSCN = 0.1 mol L^{-1} and different amounts of KOCN salt. (a) 1:4 $KAuBr_4$: NCS^- mole ratio solutions. (b) 1:4:1 $KAuBr_4$: NCS^- : NCO^- mole ratio solutions. (c) 1:4:2 $KAuBr_4$: NCS^- : NCO^- mole ratio solutions. (d) 1:4:4 $KAuBr_4$: NCS^- : NCO^- mole ratio solutions.

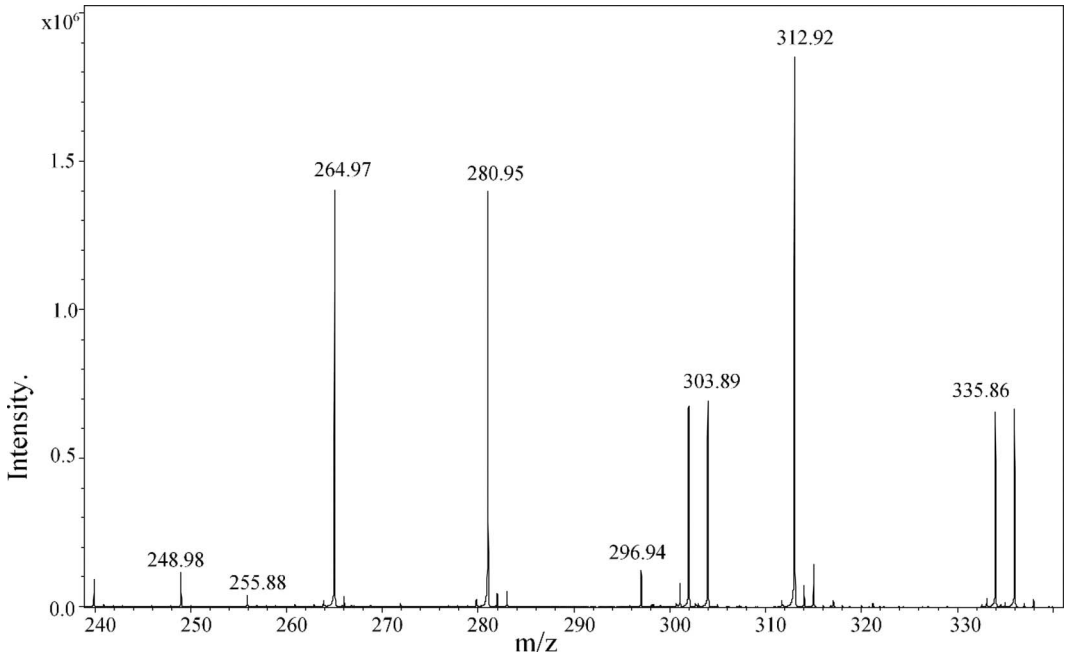

Figure 10. Electrospray mass spectra of the model solutions prepared with $KAuBr_4$ salts and pseudohalide salts in DMSO solution where $[KAuBr_4] = 0.025$ mol L^{-1}, $[NaSCN] = 0.1$ mol L^{-1} and different amounts of KOCN salt.

DMSO solution. More importantly, the broader peaks occurring over the 2234–2246 cm^{-1} range are similar in frequency and shape to the weak, broad peak observed in the in situ IR spectra of Au electrodes anodically polarized in KOCN/DMSO/TBAP electrolytes. This peak is hence assigned to an Au(I)-cyanate complex ion. The shift in peak maximum in the IR spectra in going from Fig. 9c to 9d is symptomatic of a mixed complex ion (e.g. $[Au(CN)(NCO)]^-$) being initially formed which is likely to convert to $[Au(NCO)_2]^-$ as more cyanate is added to the solution. The peak at 2234 cm^{-1} is very close in frequency to that peak observed in the in situ IR spectra as shown in Fig. 2a earlier and hence is likely to be the same solution species, i.e $[Au(NCO)_2]^-$. Given the model solution is more complex in composition than the electrolyte cell solutions discussed earlier, it is important to recognize that other species such as the mixed $[Au(CN)(NCO)]^-$ ion could also be present in the model solutions investigated.

ESMS investigations of the mixed $KAuBr_4$/NaSCN/KOCN model solutions in DMSO.—Evidence to support some of the interpretations made from the IR spectra discussed in (iv) was provided by the recording of ESI-MS spectra of the $KAuBr_4$/NaSCN (1:4 mole ratio solutions) and the mixed $KAuBr_4$/NaSCN/KOCN (1:4:4 mole ratio solutions). The typical peaks detected in the 1:4 mole ratio $KAuBr_4$:NaSCN solution were illustrated in Fig. 8b. Fig. 10 is the ESI-MS spectrum of the $KAuBr_4$/NaSCN/KOCN mixed solution. This spectrum (Fig. 10) shows 5 prominent to medium intensity mass spectral peaks. Of these, the most prominent is the $[Au(SCN)_2]^-$ ion at m/z = 312.93 which indicates this ion is still present in the mixed solution. However other ions at m/z 264.98, 280.95, 303.9 and 335.9 are due to $[Au(NCO)(CN)]^-$, ($[Au(CN)(SCN)]^-$ and $[Au(NCO)_2]^-$), $[AuBr(CN)]^-$ and $[Au(SCN)Br]^-$ respectively. The appearance of the m/z = 264.98 and 280.95 peaks due to $[Au(NCO)(CN)]^-$ and ($[Au(CN)(SCN)]^-$ and $[Au(NCO)_2]^-$) are the most significant observations as they prove the existence of Au(I) cyanate complexes in solution as intimated by the IR spectra. The m/z = 280.95 peak actually occurs in ESI-MS spectra of 1) the 1:4 mole ratio ($KAuBr_4$:NaSCN)model solution and 2) the mixed $KAuBr_4$/KOCN/NaSCN model solutions and is probably mostly due to the species $[Au(CN)(SCN)]^-$ especially so in Fig. 8b where no cyanate ion is present. However this peak could also potentially contain some contribution from an $[Au(NCO)_2]^-$ species as it has a very similar mass to $[Au(CN)(SCN)]^-$. The peak at m/z = 264.98 in Fig. 10 is, hence believed to be stronger evidence (for the presence of Au(I)-cyanate species existing in the mixed $KAuBr_4$/KOCN/NaSCN solution) than the appearance of the m/z 280.95 peak.

When a $KAuBr_4$/KSeCN/KOCN mixed solution in a 1:4:4 mole ratio was prepared and examined in similar manner by FTIR and ESI-MS (Fig. 11 and 12), identical peaks in the IR were detected which confirmed the presence of Au(I) cyanate species. In addition (in ESI-MS spectra), the same peak at m/z = 264.98 (albeit at weaker intensity) due to the mixed gold-cyanate-cyanide complex ion species was observed. Additional peaks observed in the ESI-MS spectrum (Fig. 12) of the $KAuBr_4$/KSeCN/KOCN model solution (mole ratio = 1:4:4) at m/z = 301.9/303.9, 328.90, 381.80, and 408.82, were assigned (as discussed above) to $[Au(CN)Br]^-$, $[Au(SeCN)(CN)]^-$, $[Au(SeCN)Br]^-$ and $[Au(SeCN)_2]^-$ respectively. The peak at m/z = 408.82 was the dominant peak in this ESI-MS spectrum which reflects its dominance in the mixed $KAuBr_4$/cyanate/selenocyanate model solution. In conclusion, ESI-MS spectra of these mixed model solution systems reflect a common species, namely the m/z – 264.98 peak corresponding to $[Au(NCO)(CN)]^-$ which was deemed to be a more reliable indicator of the presence of the Au(I)cyanate complex ion in these systems. This hence proves that such a species can be prepared independently of an electrochemical cell and therefore confirms that an Au(I) cyanate species has been prepared and detected in the IR spectroelectrochemical experiments.

Conclusions

SNIFTIRS studies have shown that Au electrodes undergo anodic dissolution in DMSO and DMF solutions of pseudohalide ions to form the corresponding diisocyanato-, dithiocyanato- and diselenocyanatoaurate(I) complex ion species. These are the main species formed as well as CO_2 which is detected for electrodes polarized in the presence of NCS^- and NCO^- only. Electrochemically the onset of formation of these complex ions is mostly above +500 mV (AgCl/Ag) in all systems studied. Model solution studies involving mixtures of $KAuBr_4$ and the relevant pseudohalide salt in DMSO have exhaustively proven (via the use of FTIR and ESI-MS) the assignments made for the Au(I)-pseudohalide complex ion species detected in the in situ IR studies via independent synthesis using redox chemistry occurring in the Au(III)/pseudohalide model solutions.

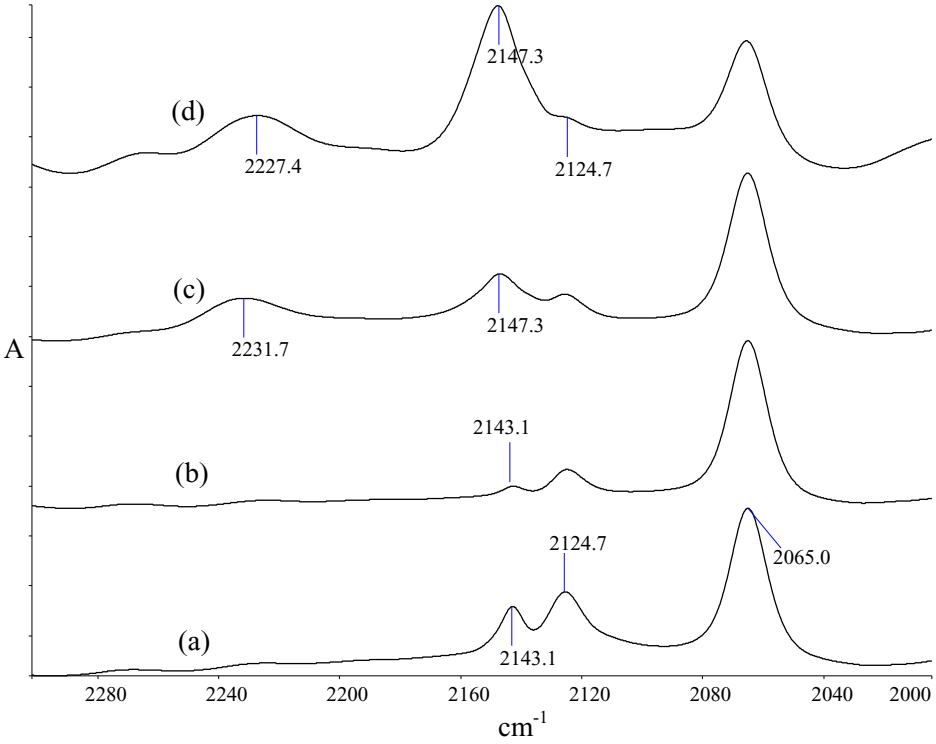

Figure 11. Transmission IR spectra of the model solutions prepared with $KAuBr_4$ salts and pseudohalide salts in DMSO solution where $KAuBr_4$ = 0.025 mol L^{-1}, KSeCN = 0.1 mol L^{-1} and different amounts of KOCN salt. (a) 1:4 $KAuBr_4$: $NCSe^-$ mole ratio solutions. (b) 1:4:1 $KAuBr_4$: $NCSe^-$: NCO^- mole ratio solutions. (c) 1:4:2 $KAuBr_4$: $NCSe^-$: NCO^- mole ratio solutions. (d) 1:4:4 $KAuBr_4$: $NCSe^-$: NCO^- mole ratio solutions.

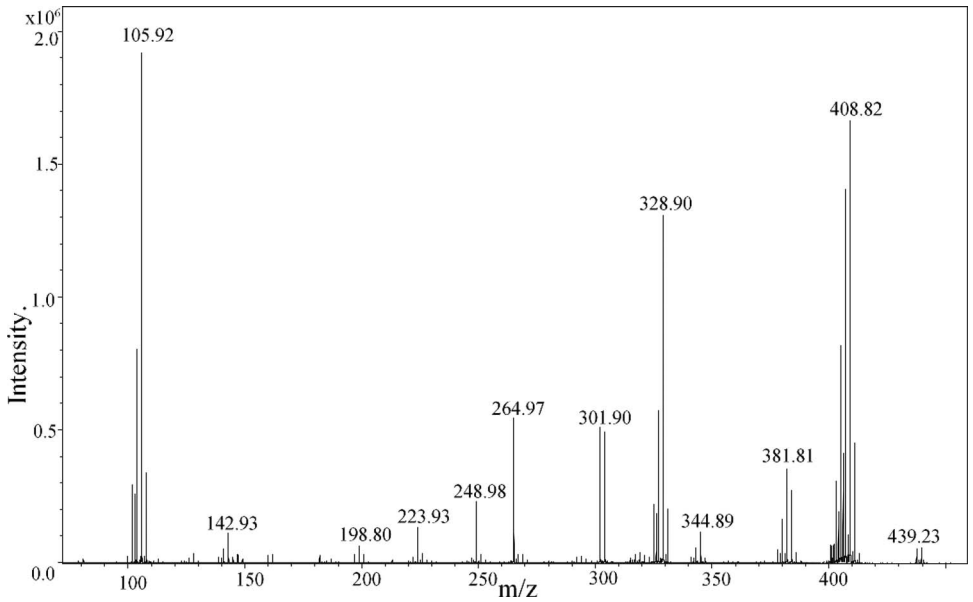

Figure 12. Electrospray mass spectra of the model solutions prepared with $KAuBr_4$ salts and pseudohalide salts in DMSO solution where [$KAuBr_4$] = 0.025 mol L^{-1}, [KSeCN] = 0.1 mol L^{-1} and different amounts of KOCN salt.

Acknowledgments

We are very grateful to Professor Bill Henderson in Chemistry for advice relating to Au(I) and Au(III) chemistry. We are also grateful to Emeritus Professor Graham Bowmaker from Auckland University for useful discussions.

References

1. J. Banas, B. Stypula, K. Banas, J. Swiatowska-Mrowiecka, M. Starowicz, and U. Lelek-Borkowska, *J. Solid State Electrochem.*, **13**(11), 1669 (2009).
2. F. Bellucci, C. A. Farina, and G. Faita, *Electrochimica Acta*, **26**, 731 (1981).
3. L. Ercolano, T. Monetta, and F. Bellucci, *Corrosion Science*, **35**, 161 (1993).
4. M. D. Adams and M. W. Johns, in *Gold Progress in Chemistry- Biochemistry and Technology*, H. Schmidbaur Editor, John Wiley & Sons (1999).
5. L. K. H. K. Alwis, M. R. Mucalo, and B. Ingham, *J. Electrochem. Soc.*, **60**, H803 (2013).
6. K. Ashley, *Talanta*, **38**(11), 1209 (1991).
7. K. Ashley and S. Pons, *Chemical Reviews*, **88**, 673 (1988).
8. G. A. Bowmaker, J.-M. Leger, A. Le Rille, C. A. Melendres, and A. Tadjeddine, *J. Chem. Soc., Faraday Trans.*, **94**(9), 1309 (1998).
9. K. Brandt, E. Vogler, M. Parthenopoulos, and K. Wandelt, *J. Electroanal. Chem.*, **570**, 47 (2004).
10. M. Bron and R. Holze, *J. Electroanal. Chem.*, **385**, 105 (1995).
11. M. Bron and R. Holze, *Electrochim. Acta.*, **45**, 1121 (1999).
12. D. S. Corrigan, P. Geo, L. H. Leung, and M. J. Weaver, *Langmuir*, **2**, 744 (1986).
13. D. S. Corrigan and M. J. Weaver, *Langmuir*, **4**, 599 (1988).
14. M. A. El-Attar, N. Xu, D. Awasabisah, D. R. Powell, and G. B. Richter-Addo, *Polyhedron*, **40**, 105 (2012).

15. C. Korzeniewski, in *Handbook of Vibrational Spectroscopy*, J. M. Chalmers and P. R. Griffiths Editors, p. 2700, John Wiley, New York (2002).
16. C. A. Melendres, G. A. Bowmaker, K. A. B. Lee, and B. Beden, *J. Electroanal. Chem.*, **449**, 215 (1998).
17. M. R. Mucalo, R. P. Cooney, and G. A. Wright, *J. Chem. Soc. Faraday Trans.*, **86**, 1083 (1990).
18. M. R. Mucalo and Q. Li, *Journal of Colloid and Interface Science*, **269**, 370 (2004).
19. D. Parry and J. M. Harris, *Langmuir*, **6**, 209 (1990).
20. M. J. Smieja, M. D. Sampson, K. A. Grice, E. A. Benson, J. D. Froehlich, and C. P. Kubiak, *Inorg. Chem.*, **52**, 2484 (2013).
21. R. M. Souto, F. Ricci, L. Spyrkowicz, J. L. Rodriguez, and E. Pastor, *J. Phys. Chem. C*, **115**, 3671 (2011).
22. N. Xu, J. Lilly, D. R. Powell, and G. B. Richter-Addo, *Organometallics*, **31**, 827 (2012).
23. Y. Y. Yang, J. Ren, H.-X. Zhang, Z.-Y. Zhou, S.-G. Sun, and W.-B. Cai, *Langmuir*, **29**, 1709 (2013).
24. B. Bozzini, M. Kazemian Abyaneh, B. Busson, G. P. de Gaudenzi, L. Gregoratti, C. Humbert, M. Amati, C. Mele, and A. Tadjeddine, *J. Power Sources*, **231** (2013).
25. C.-H. Zhen, S.-G. Sun, C.-J. Fan, S.-P. Chen, B.-W. Mao, and Y.-J. Fan, *Electrochim. Acta*, **49**, 1249 (2004).
26. M. D. Benari, G. T. Hefter, and A. J. Parker, *Hydrometallurgy*, **10**, 367 (1983).
27. M. E. Martins, C. Castellano, A. J. Calandra, and A. J. Arvfa, *J. Electroanal. Chem.*, **81**, 191 (1977).
28. M. E. Martins, C. Castellano, A. J. Calandra, and A. J. Arvfa, *J. Electroanal. Chem.*, **92**, 45 (1978).
29. T. Dickinson, A. F. Povey, and M. A. Sherwood, *J. Chem. Soc., Faraday Trans. 1*, **71**, 298 (1975).
30. S. F. Mason, *J Chem. Soc.*, 1263 (1959).
31. W. Beck, W. P. Fehlhammer, P. Poellmann, and H. Schaechl, *Chemische Berichte*, **102**(6), 1976 (1969).
32. G. A. Bowmaker and D. A. Rogers, *Journal of the Chemical Society, Dalton Transactions: Inorganic Chemistry (1972-1999)*, 9, 1873 (1982).
33. J. B. Melpolder and J. L. Burmeister, *Inorg. Chem.*, **11**, 911 (1972).
34. W. R. Mason and H. B. Gray, *Inorg. Chem.*, **7**, 55 (1968).
35. N. de Stefano and J. L. Burmeister, *Inorg. Chem.*, **10**, 998 (1971).
36. W. Henderson and J. S. McIndoe, in *Mass Spectrometry of Inorganic, Coordination and Organometallic Compounds*, p. 127, John Wiley & Sons, Ltd (2005).
37. T. Guo, L. Li, V. Cammarata, and A. Illies, *J. Phys. Chem. B*, **109**(16), 7821 (2005).
38. K. Kunimatsu, H. Seki, W. G. Golden, J. G. Gordon, and M. R. Philpott, *Langmuir*, **4**, 337 (1988).
39. A. C. Reeder and H. E. Spencer, *Journal of Imaging Science*, **31**(3), 126 (1987).
40. O. Topel, I. Persson, and E. Avsar, *J. Mol. Liq.*, **143**, 89 (2008).
41. M. Rawashdeh-Omary, M. Omary, and H. H. Patterson, *Journal of the American Chemical Society*, **122**, 10371 (2000).
42. J. Emsley, *The Elements*, Clarendon press- Oxford (1991).